

Received: 2019.12.12
Accepted: 2020.01.30
Available online: 2020.03.12
Published: 2020.03.17

Identification of Hub Genes in High-Grade Serous Ovarian Cancer Using Weighted Gene Co-Expression Network Analysis

Authors' Contribution:
Study Design A
Data Collection B
Statistical Analysis C
Data Interpretation D
Manuscript Preparation E
Literature Search F
Funds Collection G

CDE **Meijing Wu**
BF **Yue Sun**
BF **Jing Wu**
A **Guoyan Liu**

Department of Gynecology and Obstetrics, Tianjin Medical University General Hospital, Tianjin, P.R. China

Corresponding Author: Guoyan Liu, e-mail: liuguoyan211@126.com

Source of support: This work was supported by a grant from the National Natural Science Foundation of China (grant number 81472761 to GL)

Background: High-grade serous ovarian cancer (HGSOC) is the most malignant gynecologic tumor. This study reveals biomarkers related to HGSOC incidence and progression using the bioinformatics method.

Material/Methods: Five gene expression profiles were downloaded from GEO. Differentially-expressed genes (DEGs) in HGSOC and normal ovarian tissue samples were screened using limma and the function of DEGs was annotated by KEGG and GO analysis using clusterProfiler. A co-expression network utilizing the WGCNA package was established to define several hub genes from the key module. Furthermore, survival analysis was performed, followed by expression validation with datasets from TCGA and GTEx. Finally, we used single-gene GSEA to detect the function of prognostic hub genes.

Results: Out of the 1874 DEGs detected from 114 HGSOC versus 49 normal tissue samples, 956 were upregulated and 919 were downregulated. The functional annotation indicated that upregulated DEGs were mostly enriched in cell cycle, whereas the downregulated DEGs were enriched in the MAPK or Ras signaling pathway. Two modules significantly associated with HGSOC were excavated through WGCNA. After survival analysis and expression validation of hub genes, we found that 2 upregulated genes (*MAD2L1* and *PKD2*) and 3 downregulated genes (*DOCK5*, *FANCD2* and *TBRG1*) were positively correlated with HGSOC prognosis. GSEA for single-hub genes revealed that *MAD2L1* and *PKD2* were associated with proliferation, while *DOCK5*, *FANCD2*, and *TBRG1* were associated with immune response.

Conclusions: We found that *FANCD2*, *PKD2*, *TBRG1*, and *DOCK5* had prognostic value and could be used as potential biomarkers for HGSOC treatment.

MeSH Keywords: **Computational Biology • Ovarian Neoplasms • Survival Analysis**

Full-text PDF: <https://www.medscimonit.com/abstract/index/idArt/922107>



2021



5



13



37



Background

Ovarian cancer has a high mortality rate, which ranks first among gynecologic malignant tumors. Most deaths (70%) of patients presented with advanced-staged, high-grade serous ovarian cancer (HGSOC) due to the lack of specific symptoms at the early stage [1]. Therefore, it is of great significance to study the potential prognostic biomarkers related to the development of HGSOC.

In recent years, bioinformatics-assisted analyses of expression profile have been widely used to detect the biomarkers of human diseases [2]. Weighted gene co-expression network analysis (WGCNA) is a biological approach to determine highly synergistic gene sets and to identify the association between gene modules and phenotype of samples [3]. WGCNA has been comprehensively utilized in multiple cancer-associated studies to determine hub genes that could be associated with respective traits, such as pancreatic carcinoma [4], colon cancer [5], and ovarian cancer [6–10]. However, few previous studies have focused on HGSOC.

To identify potential biomarkers for specific diagnosis and therapy targets in HGSOC, WGCNA was performed to discover the hub genes that play an essential role in the development of HGSOC.

Material and Methods

Data collection

Five gene expression profiles were downloaded from the Gene Expression Omnibus (GEO) (<http://www.ncbi.nlm.nih.gov/geo/>).

Datasets GSE18520 [11], GSE27651 [12], GSE54388 [13], GSE10971 [14] and GSE14001 [15] are listed in Supplementary Table 1, with a sample size of 114 for HGSOC and 49 normal tissue samples. All samples were processed using the Affymetrix human genome U133 plus 2.0 array. Genomic and clinical data were obtained from The Cancer Genome Atlas (TCGA) (<https://cancergenome.nih.gov/>) and GTEx (<https://gtexportal.org/home/>) [16] using the TCGAbiolinks package (Version 2.14.0; <https://github.com/BioinformaticsFMRP/TCGAbiolinks>) [17]. The RNA expression profiles were sampled from 363 high-grade serous ovarian cancer and 108 normal tissues.

Research design and data preprocessing

The research design is shown in a flowchart (Figure 1). The raw data from 5 datasets were chosen for integrated analysis using the affy package (Version 3.8; <http://bioconductor.org/packages/release/bioc/html/affy.html>) [18]. The batch effect of datasets was removed using the SVA package (Version 3.8; <http://bioconductor.org/packages/release/bioc/html/sva.html>) with its combat function (Supplementary Figure 1) [19].

Differential gene expression analysis

We detected the DEGs between HGSOC and normal ovarian tissue samples using the limma package (Version 3.30.0; <http://www.bioconductor.org/packages/release/bioc/html/limma.html>) [20]. A false discovery rate (FDR) <0.05 and $|\log_2FC| > 1$ were set as the criteria value. The expression intensity and direction of DEGs were represented using the pheatmap package (Version 1.0.12, <https://cran.r-project.org/web/packages/pheatmap/>).

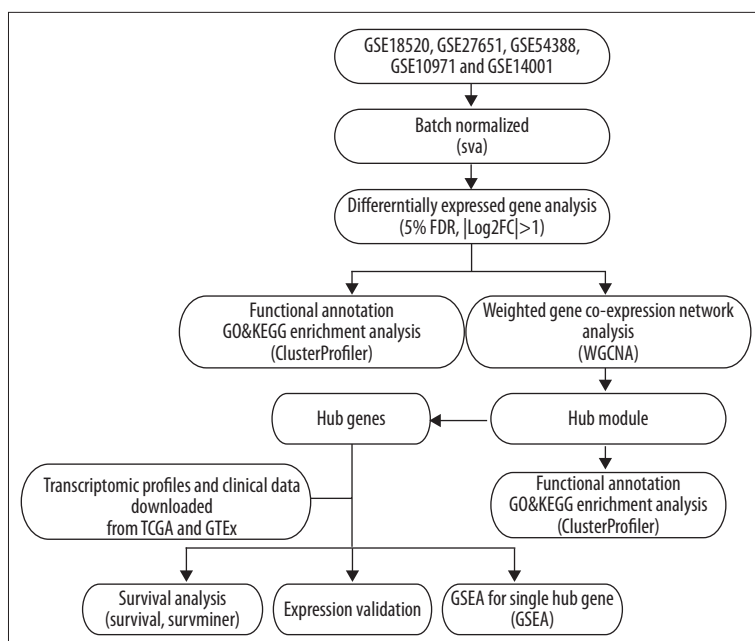


Figure 1. Flow diagram of this study.

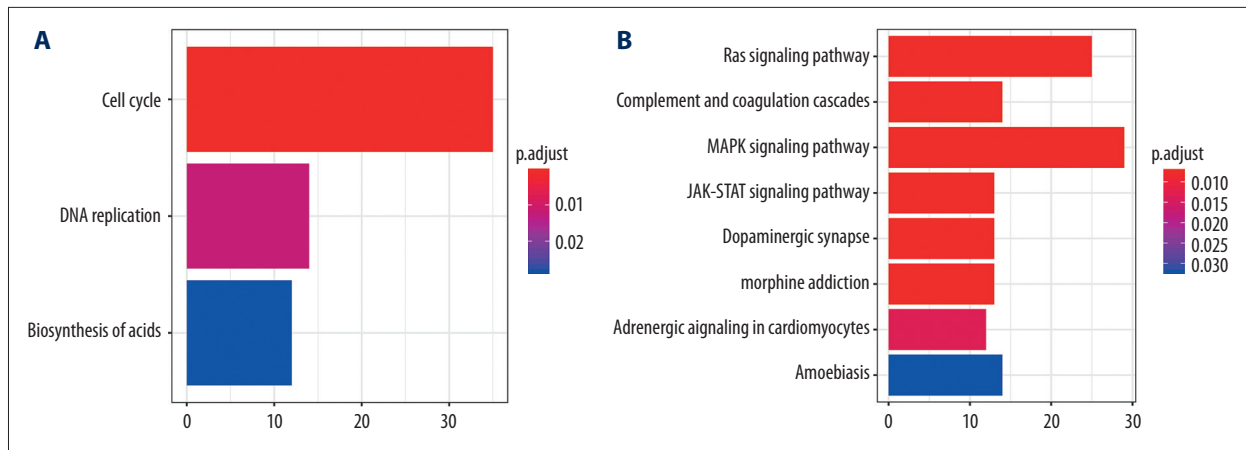


Figure 2. The KEGG pathway enrichment analysis of differently-expressed genes. **(A)** KEGG pathways enrichment for upregulated genes. **(B)** KEGG pathways enrichment for downregulated genes.

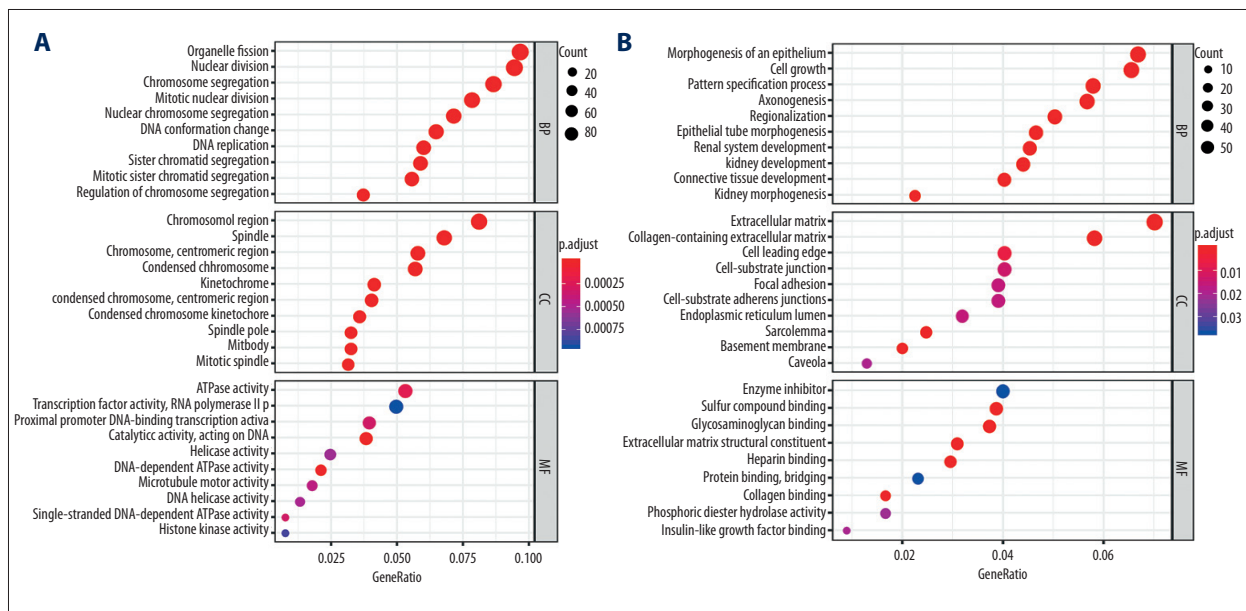


Figure 3. The GO enrichment analysis of differently-expressed genes. **(A)** GO enrichment analysis of upregulated genes. **(B)** GO enrichment analysis of downregulated genes.

Function enrichment analyses

Gene Ontology (GO) and Kyoto Encyclopedia of Genes and Genomes (KEGG) pathway analyses of DEGs were conducted using the clusterProfiler package (Version 6.8; <http://www.bioconductor.org/packages/release/bioc/html/clusterProfiler.html>) [21] to predict their underlying molecular functions. A p value of <0.05 was considered statistically significant.

Weighted gene co-expression network analysis (WGCNA)

We utilized the WGCNA package (Version 1.67; <https://cran.r-project.org/web/packages/WGCNA/index.html>) to construct a co-expression network for DEGs. To identify key modules,

soft-thresholding power was set as $\beta=9$ (scale-free $R^2=0.84$), and cut height was set as 0.25 (Supplementary Figure 2). We then explored the biological function of the modules that had the highest correlation with traits through GO and KEGG pathway analyses, and hub genes in a module were selected with $|MM|>0.85$ and $|GS|>0.3$.

Survival analysis and expression validation of hub genes

Survival analysis was performed for hub genes using the survival package (Version 2.43.3; <https://cran.r-project.org/package=survival>) and survminer package (Version 0.4.3; <https://cran.r-project.org/package=survminer>). The Kaplan-Meier curves were plotted by the expression profiles from TCGA,

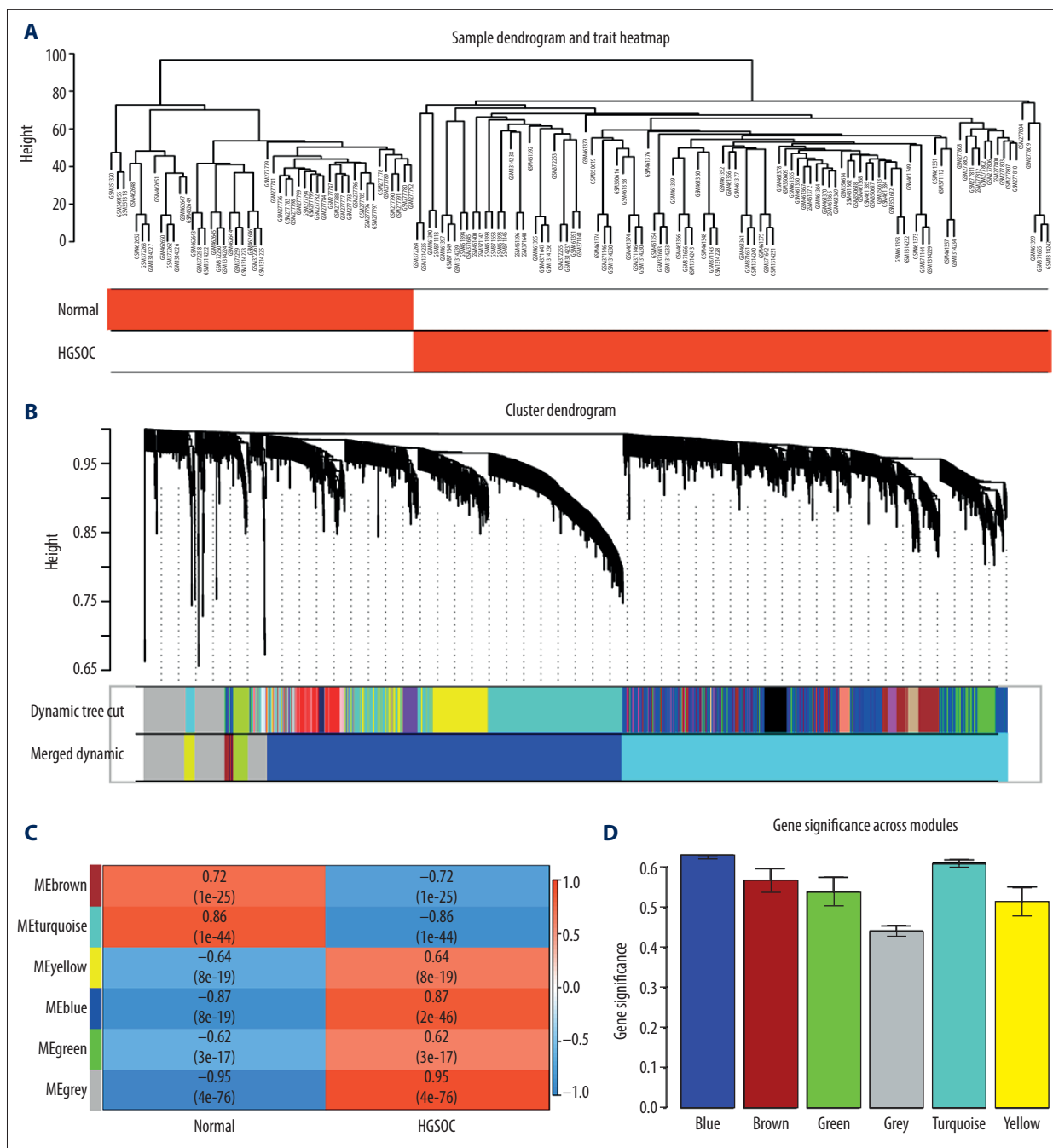


Figure 4. Co-expression modules construction and selection. **(A)** Samples clustering and trait heatmap of datasets from GEO according to the DEGs expression between HGSOc and normal tissue samples. **(B)** Dendrogram of all DEGs were clustered with dissimilarity according to topological overlap (1-TOM). **(C)** associations between modules and traits. In each cell, the upper number is the correlation coefficient of the module in the trait, and the lower number is the p value. Among them, the turquoise and blue modules were the most correlative with normal and cancer traits. **(D)** Distribution of average gene significance in the modules correlated with HGSOc. TOM – topological overlap matrix.

which were divided into 2 groups based on a certain gene's cutoff value as determined by survminer. The hub gene expression levels between HGSOc and normal tissue samples were also validated.

Gene set enrichment analysis (GSEA)

GSEA analysis of each hub gene with the TCGA-OV dataset was performed. The HGSOc samples (n=363) were divided into

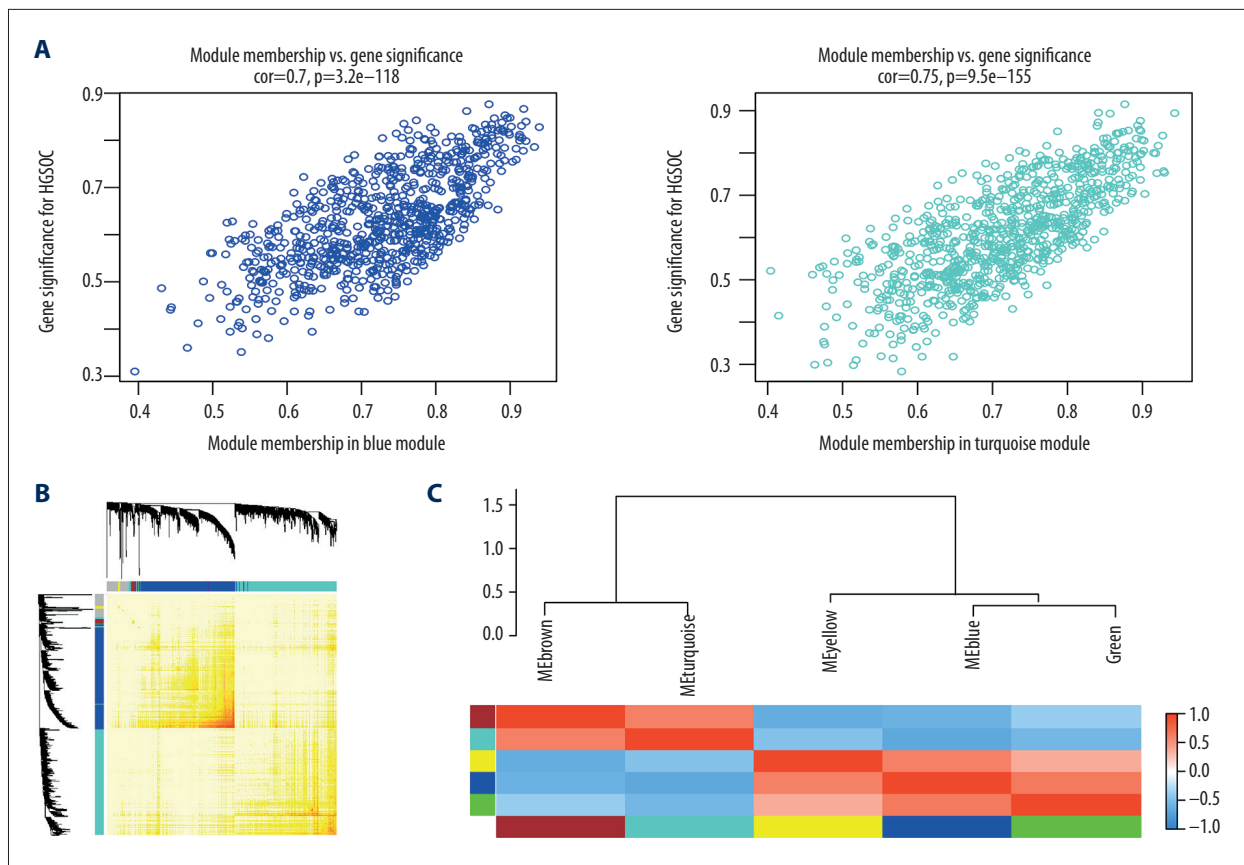


Figure 5. Select hub genes in significant co-expression modules. **(A)** The scatter plot of gene significance (GS) versus module membership (MM) in the blue module and turquoise module. **(B)** The heatmap presents the TOM among all genes. Colors beneath and right of the dendrograms explain the color-coding for each module. The more saturated yellow and red indicates a high co-expression inter-connectedness in the heatmap **(C)**. Clustering of module eigengenes and the heatmap of the adjacencies.

2 groups according to the median expression value of each hub gene (high vs. low). A p value of <0.05 was considered as statistically significant. The “h.all.v6.2.entrez.gmt” were selected as reference gene sets, which were downloaded from the Molecular Signature Database (MSigDB, <http://software.broadinstitute.org/gsea/msigdb>).

Results

Differential expression analysis

We screened 1874 DEGs, including 919 downregulated and 956 upregulated genes, between HGSOc samples and normal tissue samples. The expression changes of DEGs were represented by a heatmap (Supplementary Figure 3), which showed that the samples were divided into 2 clusters.

Function enrichment for DEGs

The potential biological functions of the upregulated and downregulated differentially-expressed genes were annotated by clusterProfiler R package. The KEGG pathway analysis revealed that the upregulated genes were mainly involved in regulation of cell cycle, DNA replication, and biosynthesis of amino acids, while the downregulated genes were mainly linked to the Ras signaling pathway, complement and coagulation cascades, and the MAPK and JAK-STAT signaling pathways (Figure 2 and Supplementary Table 2). Furthermore, we performed GO enrichment analysis, the biological progress of which was in line with the KEGG enrichment results. Chromosome segregation and mitotic nuclear division were indicated for the upregulated genes, while morphogenesis of an epithelium and collagen-containing extracellular matrix were indicated for the downregulated genes (Figure 3 and Supplementary Table 3).

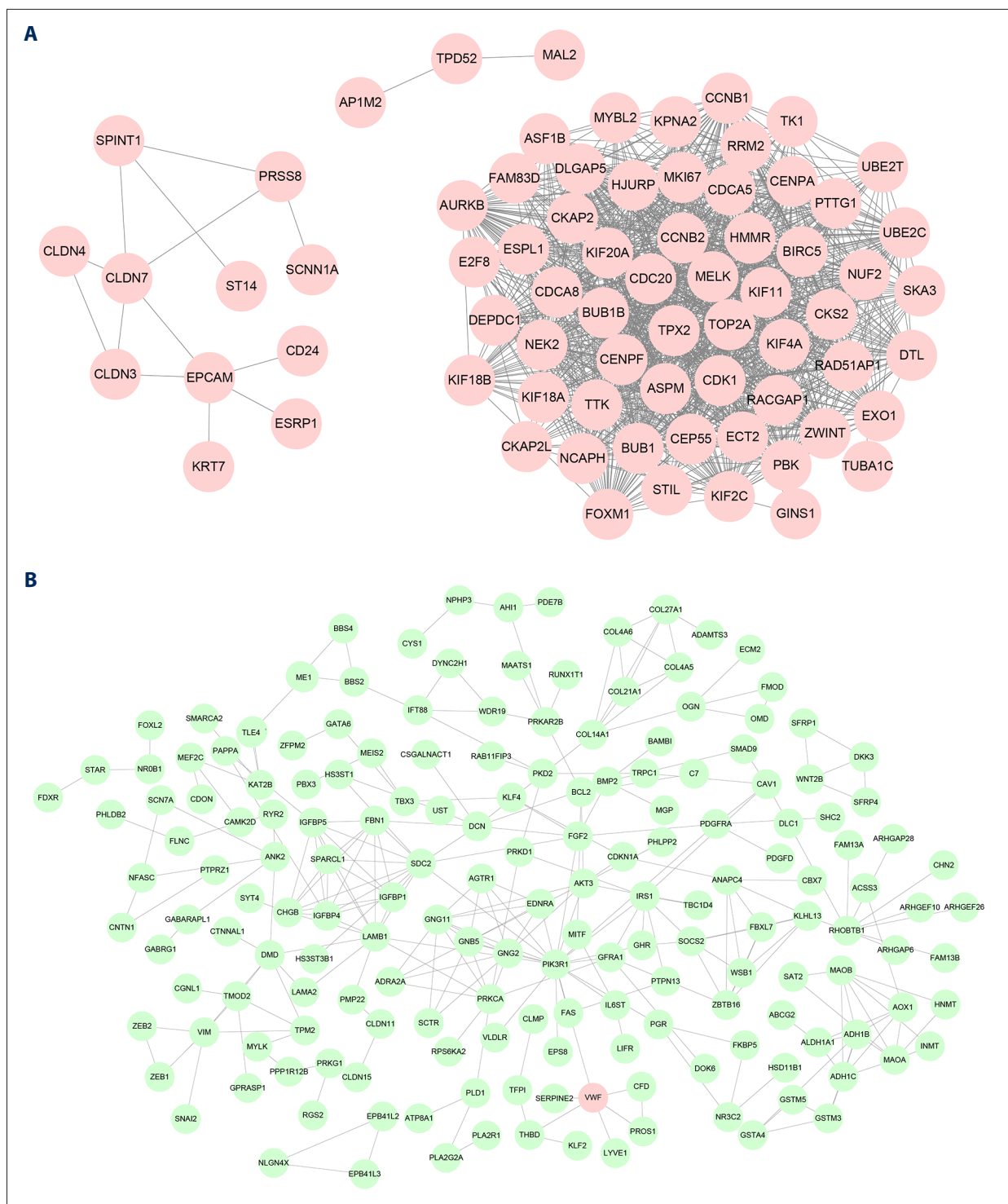


Figure 6. Protein-Protein Interaction (PPI) network of genes in 2 modules. **(A)** The genes in blue module. **(B)** The genes in turquoise module. The color presents the fold change (upregulated genes are red, downregulated genes are green).

Co-expression modules construction

To construct co-expression modules and find the key modules related to HGSOV, the expression profiles of 1874 DEGs

were assessed with the WGCNA package. Hierarchical clustering analysis is presented in Figure 4A. Then, the highly related genes were put into modules. The MED threshold was set as 0.25, and 6 modules were excavated (Figure 4B). The genes that

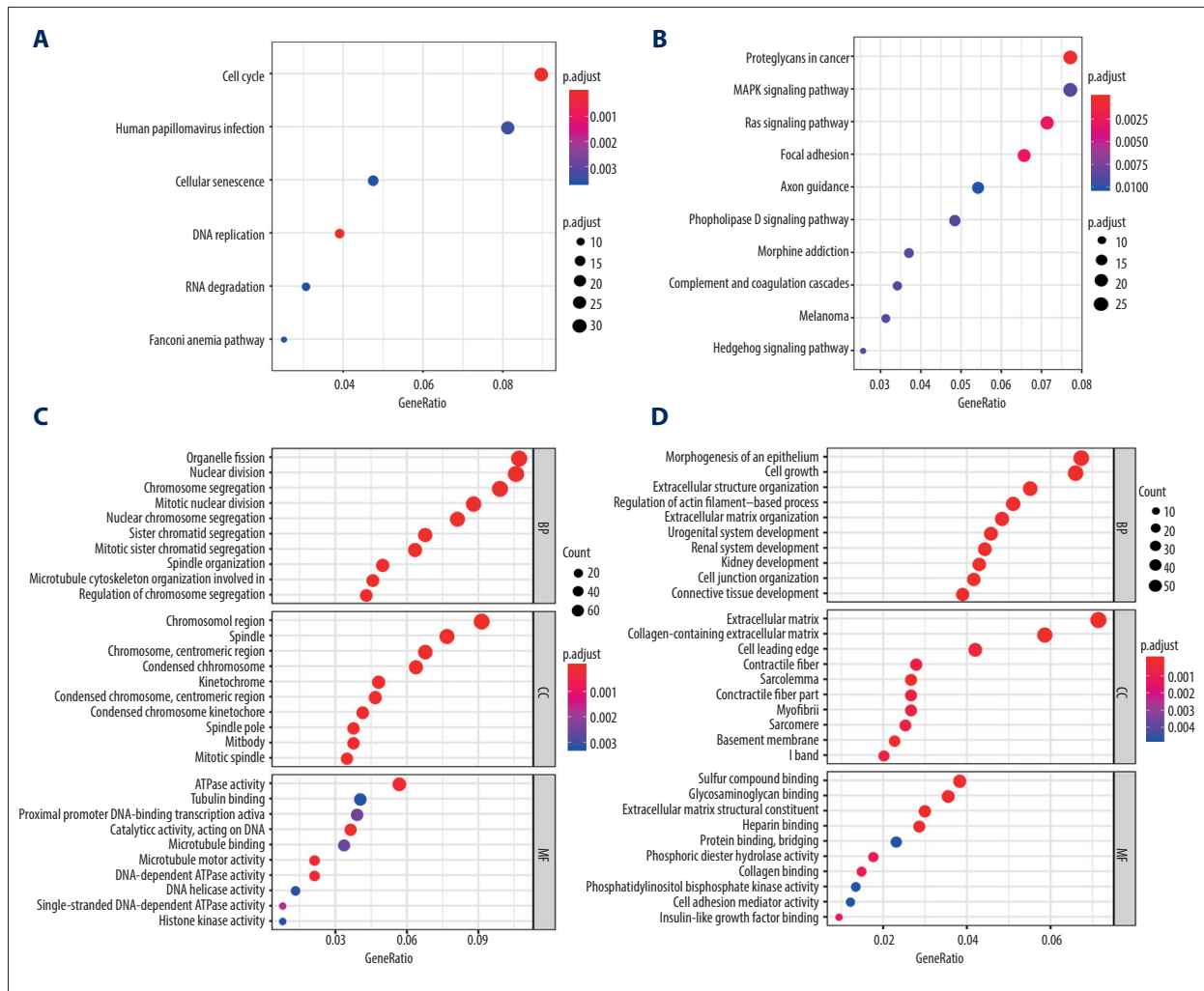


Figure 7. GO and KEGG pathway analysis of the 2 modules. (A) KEGG pathway analysis of blue module; (B) KEGG pathway analysis of turquoise module; (C) GO analysis of blue module; (D) GO analysis of turquoise module. GO analysis includes biological process (BP), cellular component (CC), and molecular function (MF). The count represents the number of genes in each pathway and dot size corresponds to “count”.

did not belong to any module were collected in the gray module, and were not used in any subsequent analysis. The other 5 modules are shown in blue, turquoise, yellow, brown, and green, respectively (Figure 4C). Among the 5 modules, the turquoise and blue modules had remarkable relevance for tumor progression (Figure 4C, 4D).

Moreover, intramodular analysis for GS and MM resulted in the identification of genes in the turquoise module, which were negatively correlated with HGSOC (correlation=0.75 and $p < 9.5 \times 10^{-155}$) and genes in the blue module revealed a highly positive correlation with HGSOC (correlation=0.7 and $p < 3.2 \times 10^{-118}$), as shown in Figure 5A.

The heatmap was plotted to show all genes (Figure 5B). To quantify co-expression similarity of the 5 modules, we

calculated the connectivity of eigengenes. Positively correlated eigengenes were grouped together, with 2 of 5 modules were classified into one cluster and 3 into another. The heatmap of the adjacencies is also presented (Figure 5C).

There were 76 hub genes from the turquoise module and 76 hub genes from the blue module selected, with a threshold module membership (MM) > 0.85 and gene significance (GS) > 0.3 (Supplementary Table 4).

The turquoise and blue modules were analyzed by STRING database, with a combined score > 0.7 and were visualized by Cytoscape software (Figure 6).

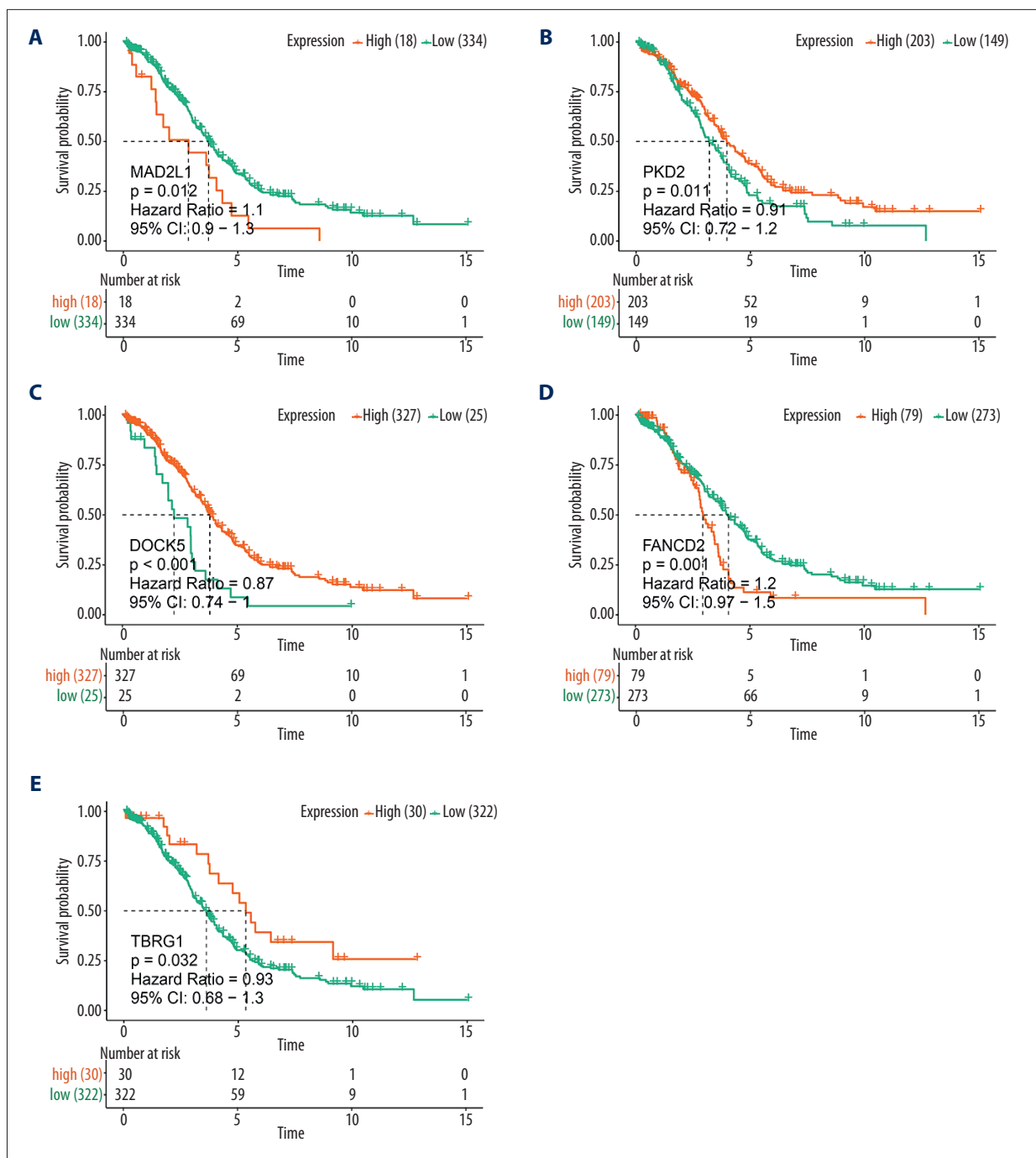


Figure 8. Kaplan-Meier analysis of (A) *MAD2L1*, (B) *PKD2*, (C) *DOCK5*, (D) *FANCD2*, and (E) *TBRG1* by comparing the higher (red) and lower (green) expressions with overall survival outcomes for patients with HGSOc.

To investigate the potential functions of the genes within the 2 modules (turquoise and blue), we performed GO and KEGG pathway analyses, and showed the most significant GO terms and KEGG pathways in Figure 7. This analysis revealed that genes in the blue module were mainly enriched in cell cycle and DNA replication, while genes in the turquoise module played their roles in different signal pathways.

Validation of hub genes

Analyzing the results of WGCNA, we found that the turquoise and blue modules had the highest association with HGSOc. Accordingly, we hypothesized that the genes in the turquoise module might act as tumor suppressors and genes in the blue module might act as tumor promoters. Survival analyses were

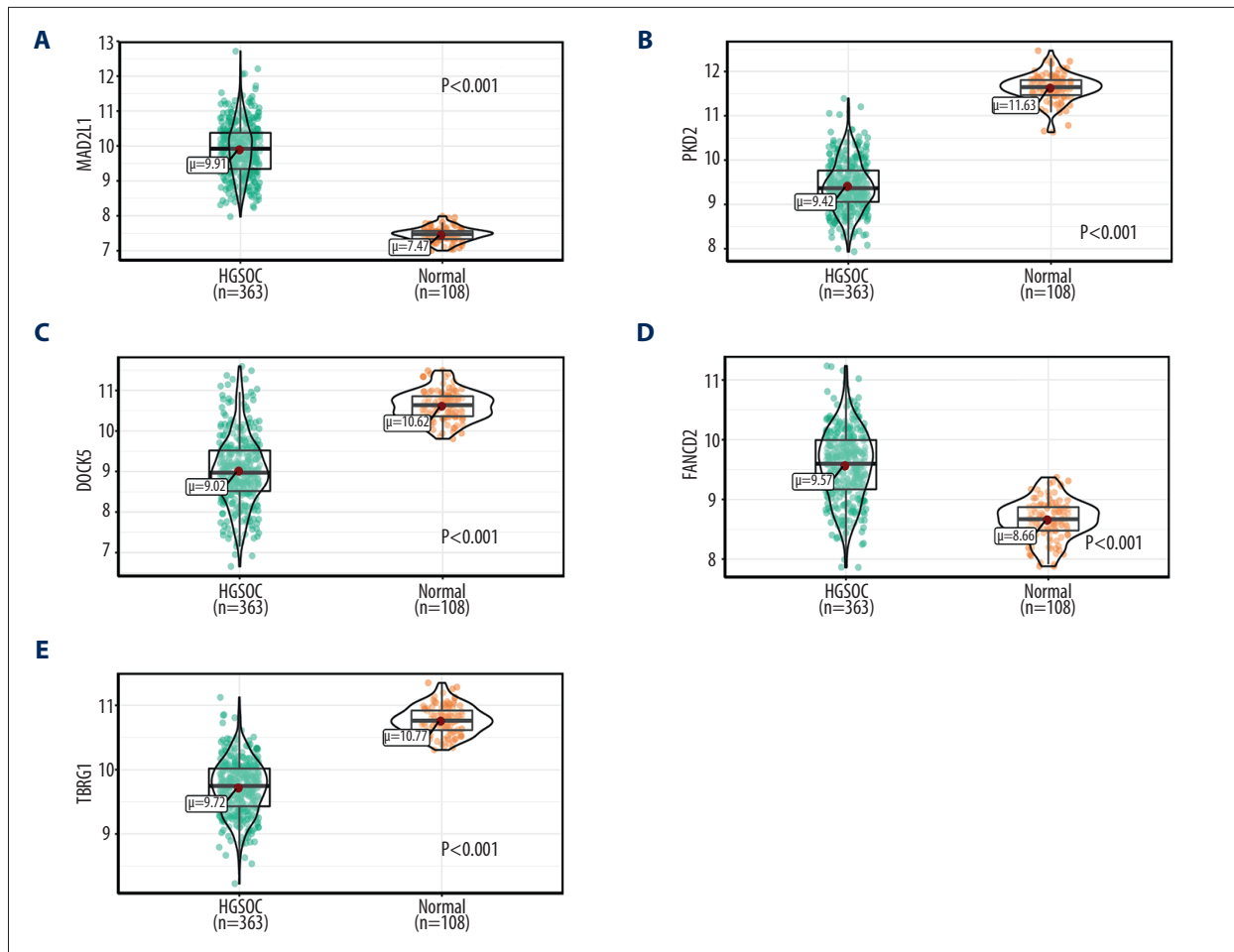


Figure 9. Validation of hub gene expressions in the TCGA and GTEx datasets. (A) *MAD2L1*, (B) *PKD2*, (C) *DOCK5*, (D) *FANCD2*, and (E) *TBRG1* gene expression differences between HGSOV and normal tissues.

performed among the 152 hub genes selected from the 2 modules. We found that *MAD2L1* and *FANCD2* in the blue module and *PKD2*, *TBRG1*, and *DOCK5* in the turquoise module were consistent with our speculation. Survival curves showed that higher expression of *MAD2L1* and *FANCD2* was significantly associated with poor prognosis of patients, as was the lower expression of *PKD2*, *TBRG1*, and *DOCK5* (Figure 8). Finally, we used gene profiles downloaded from TCGA and GTEx to validate the expression of these genes, and the results were similar to the expression exhibited by GEO (Figure 9).

Potential function of hub genes through GSEA

To better understand the potential biological functions of *MAD2L1*, *FANCD2*, *PKD2*, *TBRG1*, and *DOCK5* in HGSOV, we performed GSEA based on the TCGA-OV dataset. As shown in Figure 10, genes in higher-expression groups of *MAD2L1* and *FANCD2* were all involved in “E2F TARGETS” and “G2M CHECKPOINT” of the cell cycle, which indicated that these 2 up-regulated genes are closely associated with tumor proliferation,

whereas “TNFA SIGNALING VIA NFKB”, “interferon gamma RESPONSE” and “inflammatory response” were enriched in the *PKD2*, *TBRG1*, and *DOCK5* high-expression groups, which indicated these downregulated genes are involved in immune response (Supplementary Table 5).

Discussion

With the purpose of identifying the molecular mechanism of HGSOV and to investigate potential biomarkers for better detection and therapy, we integrated the gene expression profiles of GSE54388, GSE27651, GSE10971, GSE18520, and GSE14001, which contained 114 samples of HGSOV tissue and 49 samples of normal tissue.

We identified 1874 DEGs that were correlated with HGSOV, and the cutoff criteria were $p < 0.05$ and $|\log_{2}FC| \geq 1$. In KEGG analysis, the upregulated genes were predominantly involved in cell cycle and DNA replication, while the downregulated genes

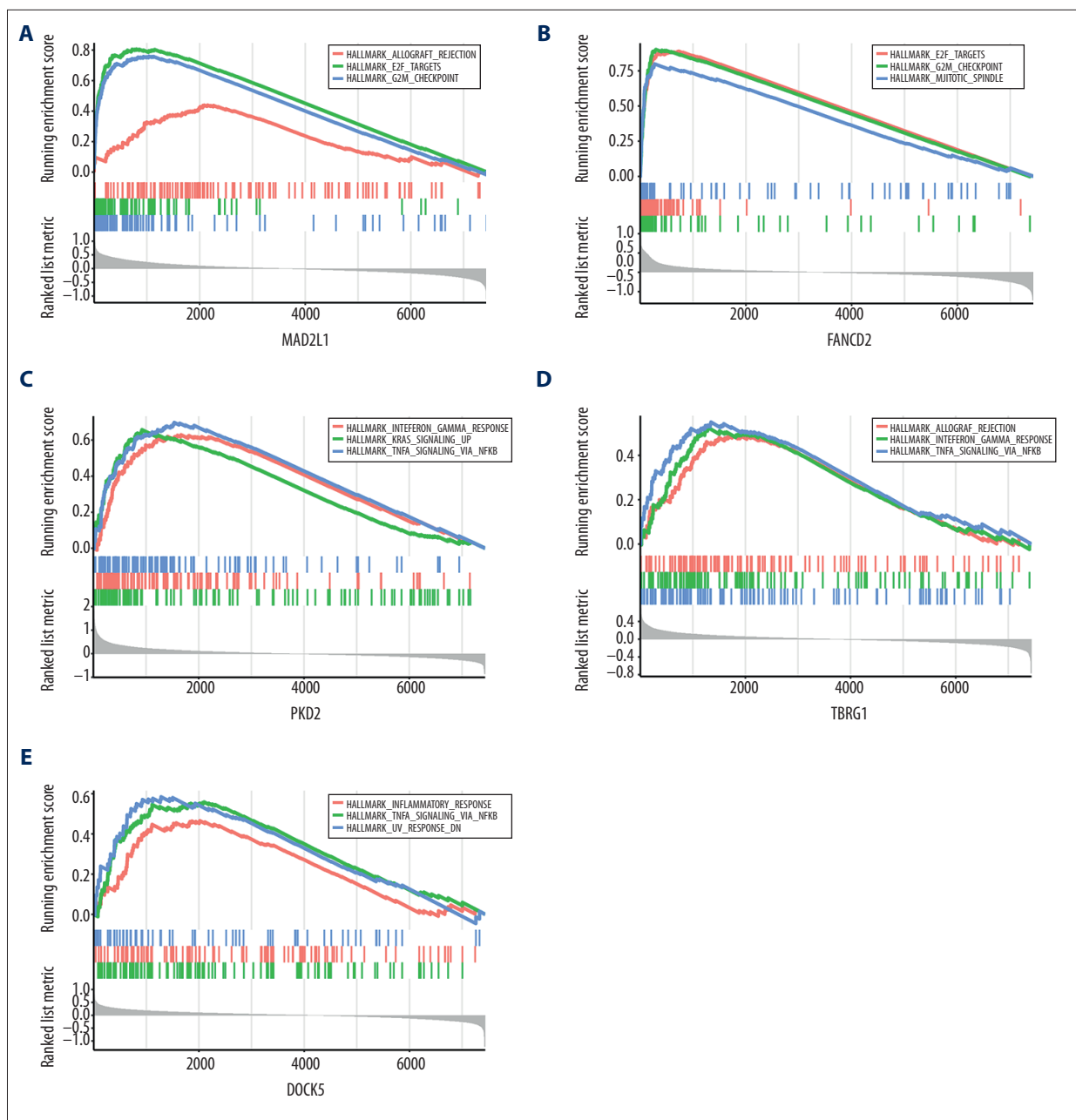


Figure 10. Gene set enrichment analysis (GSEA) of hub genes in the TCGA-OV dataset. Three gene sets enriched in the high-expressed group of single-hub genes. (A) *MAD2L1*, (B) *FANCD2*, (C) *PKD2*, (D) *TBRG1*, and (E) *DOCK5*.

were highly involved in Ras signaling, complement and coagulation cascades, and MAPK signaling pathways. The GO analysis supported the previous enrichment analysis, which both help to understand the role of DEGs in HGSOc.

WGCNA analysis was used to select co-expression modules related to the development of HGSOc, and 2 modules (blue and turquoise) were found to have the highest correlation with HGSOc. We showed the Protein-Protein Interactions (PPI) network and also performed GO and KEGG analyses for genes in the

2 modules. The results indicated that genes in the blue module were enriched in cell cycle and DNA replication, while genes in the turquoise module were involved in different signaling pathways. After filtering with MM and GS value, we detected 152 hub genes from the 2 modules. Five genes – *MAD2L1* and *FANCD2* in the blue module and *PKD2*, *TBRG1*, and *DOCK5* in the turquoise module – were excavated after survival analysis and expression validation with datasets downloaded from TCGA, and were found to have prognostic value for HGSOc. Among these 5 hub genes, *MAD2L1* and *FANCD2* are associated with ovarian cancer.

As a component of the mitotic checkpoint, high levels of *MAD2L1* are related to increased cellular proliferation, migration, and metastasis, which can lead to shorter survival in various cancers [22–26]. However, in ovarian cancer, the role of *MAD2L1* did not agree with previous findings that patients with lower *MAD2L1* levels were less sensitive to paclitaxel and had shorter progression-free survival (PFS) and overall survival (OS) [27,28]. This discrepancy might have been caused by our analysis, ignoring the mutations of *p53* and *BRCA1*, which are known regulators of *MAD2L1* and are commonly mutated in HGSOC [29,30].

High *FANCD2* levels have been shown to be associated with poor prognosis in many types of cancer [31–35], as well as in ovarian cancer [36]. *FANCD2* overexpression can stabilize the replication fork, and create *BRCA1/2* mutant tumor resistance towards *PARP1/2* inhibitor treatments [37]. The results indicated that *FANCD2* expression can influence cancer sensitivity to *PARP1/2* inhibitors and thus could be used as a potential target of therapy.

To further explore the biological functions of the 5 selected hub genes, we conducted single-gene GSEA. “E2F TARGETS” and “G2M CHECKPOINT” were enriched in the high-expression groups of *MAD2L1* and *FANCD2*, indicating their contribution to HGSOC proliferation. In the high-expression groups of *PKD2*,

TBRG1, and *DOCK5*, immune-related signals, such as “TNFA SIGNALING VIA NFKB”, “INTERFERON GAMMA RESPONSE” and “INFLAMMATORY RESPONSE” were enriched, indicating the activity of immune response.

Conclusions

We identified several DEGs and meaningful gene modules in HGSOC. Four valuable hub genes (*FANCD2*, *PKD2*, *TBRG1*, and *DOCK5*) were strongly dysregulated in HGSOC tissues. GSEA further suggested that *FANCD2* is associated with tumor proliferation, while *PKD2*, *TBRG1*, and *DOCK5* influence immune response. More work is needed to fully reveal their individual contributions towards the pathogenesis of HGSOC and to validate their value as prognostic biomarkers.

Limitations of this study include the lack of analysis for detailed clinical classification of HGSOC, such as grade, stage, lymph node metastasis, and prognosis. In future research, we will explore hub genes and their potential function based on this clinical information in detail.

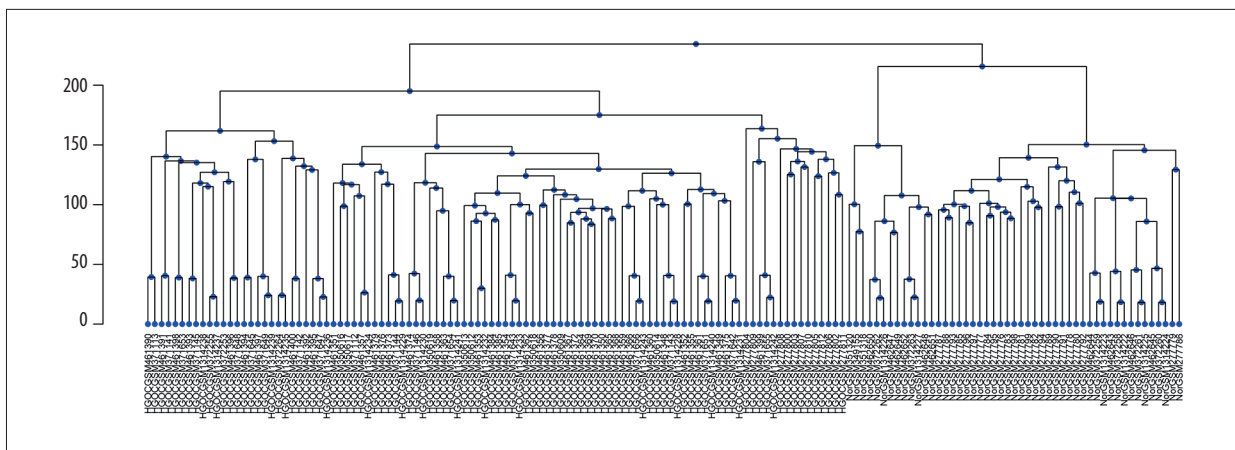
Conflict of interest

None.

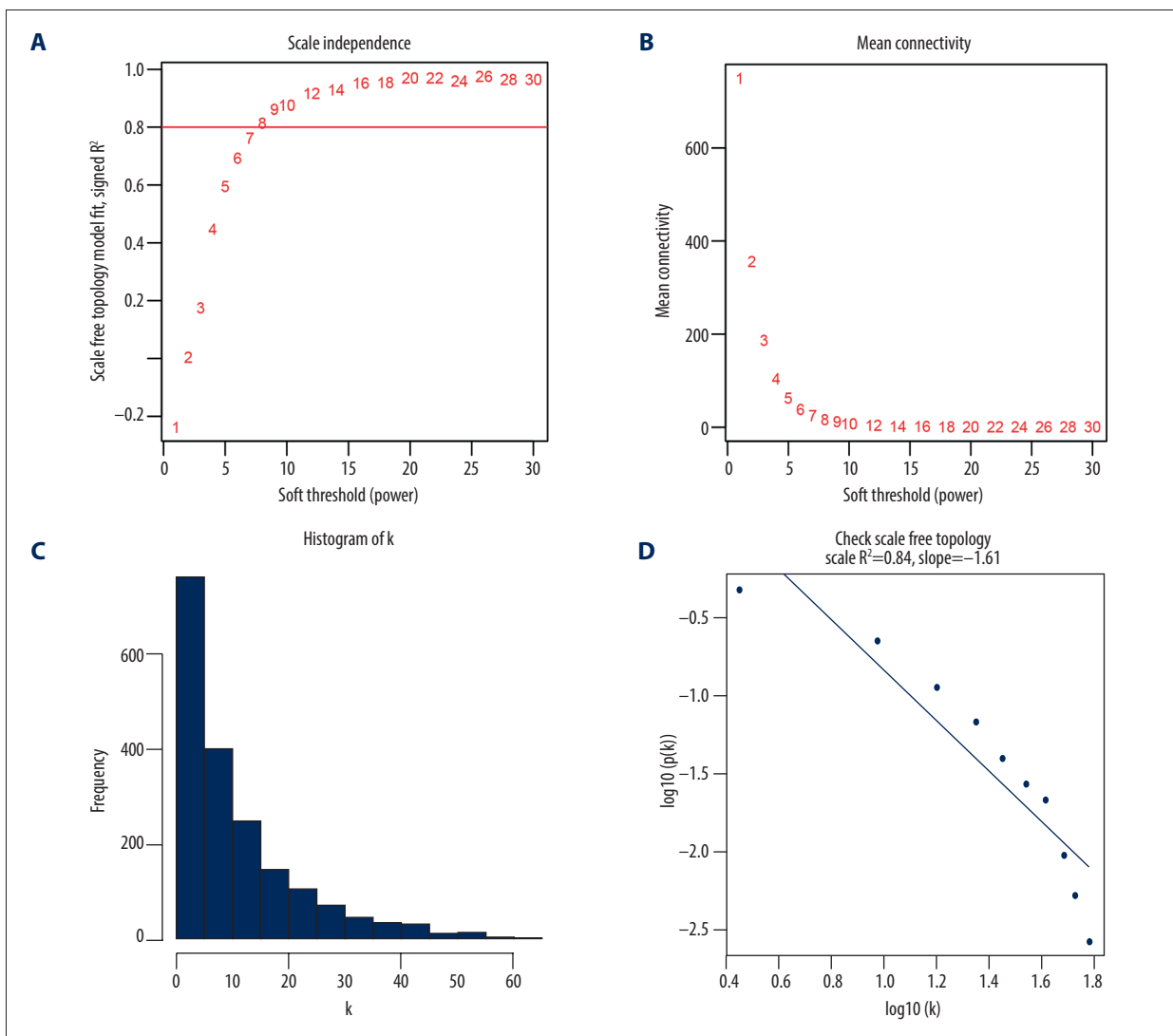
Supplementary Data

Supplementary Table 1. Characteristics of the included datasets.

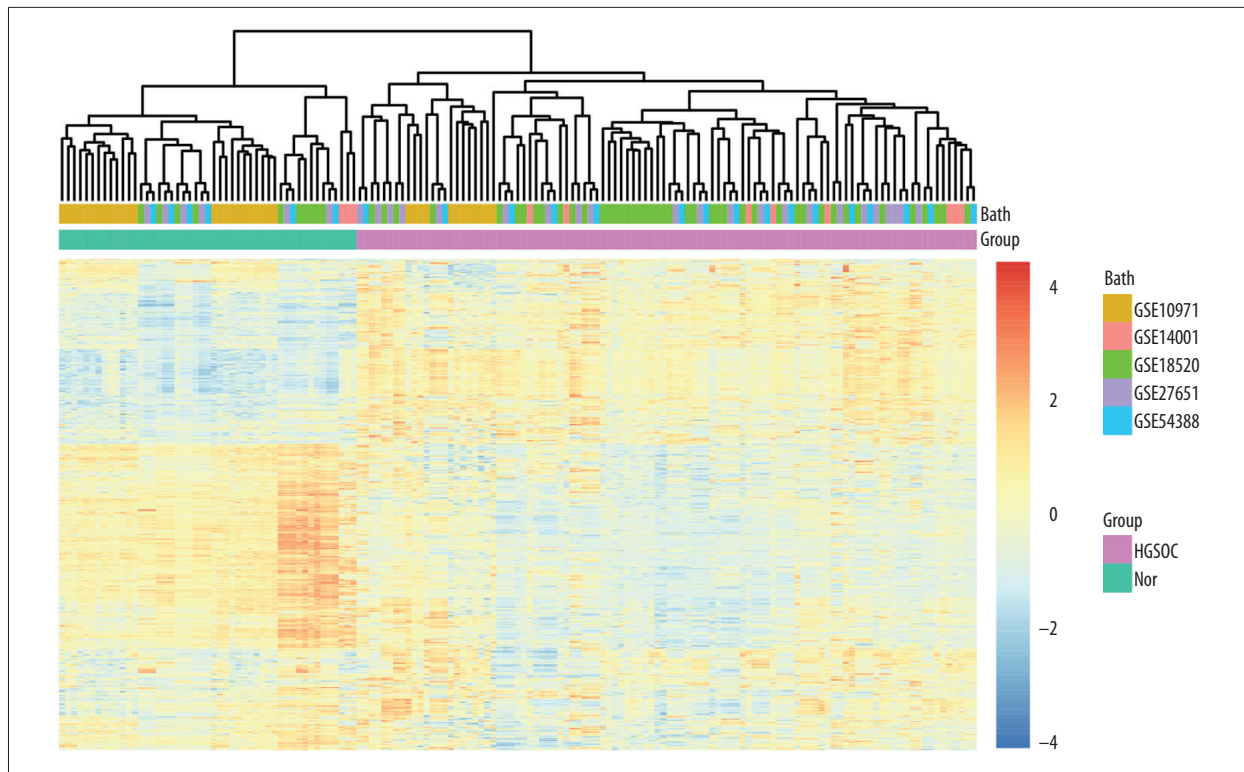
Dataset ID	GPL ID	High-grade serous ovarian carcinoma	Normal ovarian surface epithelium
GSE18520	GPL570	53	10
GSE27651	GPL570	22	6
GSE54388	GPL570	16	6
GSE10971	GPL570	13	24
GSE14001	GPL570	10	3



Supplementary Figure 1. Samples clustering of 5 datasets after removing the batch effects.



Supplementary Figure 2. Soft-thresholding power determination in WGCNA. (A) Analysis of the scale-free fit index for different soft-thresholding powers. (B) Mean connectivity for various soft-thresholding powers. (C) Histogram of connectivity distribution when $\beta=9$. (D) Check scale-free topology when $\beta=9$.



Supplementary Figure 3. Heatmap of the top 200 DEGs based on the value of $|\log FC|$. High or low expression is shown as a red or blue strip, respectively. The experimental group was labelled HGSOC, while the control group was named Nor.

Supplementary Table 2. The KEGG enrichment analysis of genes.

ID	Description	p. adjust	Count	Regulation
hsa04110	Cell cycle	0.000633	35	up
hsa03030	DNA replication	0.012093	14	up
hsa01230	Biosynthesis of amino acids	0.028478	12	up
hsa04014	Ras signaling pathway	0.007503	25	down
hsa04610	Complement and coagulation cascades	0.007503	14	down
hsa04010	MAPK signaling pathway	0.007503	29	down
hsa04630	JAK-STAT signaling pathway	0.007503	13	down
hsa04728	Dopaminergic synapse	0.007503	13	down
hsa05032	Morphine addiction	0.007503	13	down
hsa04261	Adrenergic signaling in cardiomyocytes	0.013251	12	down
hsa05146	Amoebiasis	0.03213	14	down

Supplementary Table 3. The GO enrichment analysis of genes.

Ontology	ID	Description	p. adjust	Count	Regulation
BP	GO: 0007059	Chromosome segregation	7.51E-30	76	up
BP	GO: 0140014	Mitotic nuclear division	8.88E-28	69	up
BP	GO: 0000280	Nuclear division	1.11E-26	83	up
BP	GO: 0048285	Organelle fission	3.71E-25	85	up
BP	GO: 0098813	Nuclear chromosome segregation	5.13E-25	63	up
CC	GO: 0098687	Chromosomal region	1.26E-26	74	up
CC	GO: 0000775	Chromosome, centromeric region	2.73E-24	53	up
CC	GO: 0000793	Condensed chromosome	1.10E-20	52	up
CC	GO: 0000779	Condensed chromosome, centromeric region	2.30E-19	37	up
CC	GO: 0005819	Spindle	2.30E-19	62	up
MF	GO: 0140097	Catalytic activity, acting on DNA	2.32E-08	34	up
MF	GO: 0008094	DNA-dependent ATPase activity	1.57E-05	19	up
MF	GO: 0016887	ATPase activity	0.000226	47	up
MF	GO: 0043142	Single-stranded DNA-dependent ATPase activity	0.000325	7	up
MF	GO: 0001077	Proximal promoter DNA-binding transcription activator activity, RNA polymerase II-specific	0.000325	35	up
BP	GO: 0002009	Morphogenesis of an epithelium	9.98E-07	53	down
BP	GO: 0016049	Cell growth	2.29E-06	52	down
BP	GO: 0001822	Kidney development	6.68E-06	35	down
BP	GO: 0072001	Renal system development	6.68E-06	36	down
BP	GO: 0003002	Regionalization	6.68E-06	40	down
CC	GO: 0062023	Collagen-containing extracellular matrix	1.22E-11	49	down
CC	GO: 0031012	Extracellular matrix	1.29E-10	59	down
CC	GO: 0042383	Sarcolemma	3.36E-05	21	down
CC	GO: 0005604	Basement membrane	3.64E-05	17	down
CC	GO: 0031252	Cell leading edge	0.006422	34	down
MF	GO: 0005201	Extracellular matrix structural constituent	4.99E-05	24	down
MF	GO: 0005539	Glycosaminoglycan binding	5.13E-05	29	down
MF	GO: 1901681	Sulfur compound binding	6.67E-05	30	down
MF	GO: 0008201	Heparin binding	0.000129	23	down
MF	GO: 0005518	Collagen binding	0.000836	13	down

Supplementary Table 4. Hub genes in blue and turquoise module ($|MM|>0.85$ and $|GS|>0.3$).

Gene	Blue module		Gene	Turquoise module	
	MM	GS		MM	GS
CSE1L	0.885182	0.654936	LRRN4	0.863969	-0.76695
PCNA	0.853268	0.634531	LINC01105	0.85413	-0.83749
HNRNPAB	0.859002	0.665006	DAB2	0.928442	-0.84279
TOP2A	0.891679	0.822887	CELF2	0.888927	-0.77641
SMC4	0.917093	0.806692	LAMA4	0.850672	-0.68463
MTHFD2	0.877458	0.806098	SPOCK1	0.867854	-0.80181
PSRC1	0.871528	0.788497	PAPSS2	0.879786	-0.72486
CKS1B	0.934063	0.787083	DAPK1	0.899065	-0.7982
MCM2	0.922548	0.841694	PROCR	0.898493	-0.7677
PCLAF	0.899258	0.817579	PKD2	0.929768	-0.75857
CRABP2	0.87272	0.877783	GSDME	0.91672	-0.80166
CCNB2	0.897672	0.848503	IGFBP6	0.892364	-0.79082
LSM4	0.871655	0.664114	THBD	0.869457	-0.80323
CDC20	0.893728	0.758763	KDR	0.884189	-0.74272
UBE2C	0.876499	0.834623	FRY	0.899738	-0.80017
CDK1	0.876549	0.8119	GNG11	0.930805	-0.75466
EZH2	0.862178	0.795034	ABCA8	0.944703	-0.89654
MAD2L1	0.889283	0.76929	GPRASP1	0.899009	-0.87775
PTTG1	0.870574	0.824798	GFPT2	0.866683	-0.7817
BUB1B	0.892962	0.819369	RNASE4	0.903103	-0.80729
DLGAP5	0.877017	0.82571	CALB2	0.897513	-0.85688
ZWINT	0.922712	0.79987	BCHE	0.922752	-0.81917
TRIP13	0.884367	0.77344	NPY1R	0.882911	-0.85536
RAD51AP1	0.858395	0.802612	GHR	0.888245	-0.71151
NDC80	0.86773	0.721595	ECM2	0.850415	-0.66158
CKS2	0.94052	0.829763	ARHGAP6	0.869659	-0.73929
KIF11	0.885283	0.822206	WNT2B	0.877108	-0.80996
NEK2	0.89035	0.839637	PTGIS	0.883089	-0.79366
KIF23	0.853223	0.7629	LGALS2	0.85777	-0.75854
FEN1	0.909533	0.760884	MAF	0.898868	-0.73781
TTK	0.894859	0.855031	SYNE1	0.854181	-0.8207
MELK	0.900554	0.813158	PLPP1	0.920489	-0.7545
STIL	0.867957	0.835405	TCEAL2	0.877183	-0.81491
SAC3D1	0.874805	0.712282	TBC1D2B	0.862424	-0.70643

Supplementary Table 4 continued. Hub genes in blue and turquoise module ($|MM| > 0.85$ and $|GS| > 0.3$).

Gene	Blue module		Gene	Turquoise module	
	MM	GS		MM	GS
HMGA1	0.869641	0.806441	PDE8B	0.878248	-0.91687
GIN51	0.893705	0.7861	ATP10D	0.88824	-0.74775
CENPF	0.880011	0.84842	TFPI	0.86169	-0.75802
AURKA	0.914224	0.801243	CHN2	0.855714	-0.81706
EIF4G1	0.869979	0.737708	BICC1	0.864204	-0.82881
NR2F6	0.887103	0.752212	DIXDC1	0.858203	-0.8161
BUB1	0.913764	0.809106	DIRAS3	0.875531	-0.8524
PUF60	0.866461	0.739985	OLFML1	0.886786	-0.70603
TPX2	0.862716	0.819783	CSGALNACT1	0.90082	-0.83324
RPL39L	0.857416	0.742065	PDGFD	0.866505	-0.68393
EIF6	0.86057	0.671087	RADX	0.868631	-0.84742
XPOT	0.857586	0.684634	KLF2	0.894365	-0.78132
SCRIB	0.867393	0.771012	SMPD3	0.867973	-0.78767
CCNA2	0.868501	0.7858	PPP1R3B	0.85511	-0.72434
CCNB1	0.904717	0.755995	OGN	0.88218	-0.80725
PRC1	0.886914	0.802267	ABI3BP	0.872052	-0.78816
MRPL15	0.853847	0.663766	ITLN1	0.884383	-0.81818
NUSAP1	0.867073	0.795277	MGARP	0.903375	-0.8306
SLC52A2	0.868392	0.803613	ARHGAP18	0.918993	-0.80114
TACC3	0.875177	0.752928	DDR2	0.852443	-0.67497
KIF4A	0.871167	0.797892	ANTXR2	0.858928	-0.72284
CEP55	0.850744	0.827425	LIX1L	0.878142	-0.68937
DTL	0.865255	0.780689	MCC	0.870811	-0.71797
KIF20A	0.888407	0.82511	TBRG1	0.85824	-0.79791
CENPU	0.863996	0.732426	PTPN21	0.863405	-0.7201
KIF15	0.882733	0.786989	CNRIP1	0.889837	-0.80871
ECT2	0.916732	0.831958	PPM1K	0.895422	-0.86713
CDCA8	0.85916	0.797452	MEDAG	0.866729	-0.84797
MCM4	0.914084	0.813176	LINC01279	0.857322	-0.66728
RACGAP1	0.918941	0.779139	PLEKHH2	0.865982	-0.76522
PSAT1	0.854015	0.826163	SLC30A4	0.904509	-0.70542
UBE2T	0.850996	0.725215	TCEAL3	0.856911	-0.7193
SLC25A33	0.868987	0.6974	CDON	0.869831	-0.69303
CDCA3	0.857304	0.797015	TCEAL7	0.870405	-0.84944

Supplementary Table 4 continued. Hub genes in blue and turquoise module ($|MM|>0.85$ and $|GS|>0.3$).

Blue module			Turquoise module		
Gene	MM	GS	Gene	MM	GS
NUF2	0.91985	0.868254	ERN1	0.880253	-0.77167
RCC2	0.909521	0.783731	MUM1L1	0.899449	-0.85402
FAM83D	0.901393	0.849648	RNASEL	0.872061	-0.72795
POC1A	0.856044	0.816551	DOCK5	0.893588	-0.83622
DEPDC1B	0.854264	0.764695	RBMS3	0.850965	-0.82463
CENPL	0.857368	0.768059	HAND2-AS1	0.858159	-0.89488
KIF14	0.902918	0.830047	DTWD1	0.879321	-0.75556
FANCD2	0.890071	0.736399	IFFO1	0.857298	-0.73892

MM – module membership; GS – gene significance.

Supplementary Table 5. The Gene Set Enrichment Analysis (GSEA) of hub genes.

	Description	setSize	enrichmentScore	NES	p.adjust	core_enrichment
MAD2L1	ALLOGRAFT REJECTION	120	0.438738	1.761702	0.007716	CDKN2A/NME1/GZMB/MMP9/CXCL9/CCL5/CXCL13/IL15/CCL11/EIF5A/TAP1/CCL13/GZMA/SRGN/IL2RG/CCL2/UBE2N/CCL7/HLA-DOB/CTSS/CCL4/B2M/CD3D/PRF1/CD2/LTB/TNF/SIT1/IL2RA/CD7/HLA-G/CD8A/CD3E/ST8SIA4/CD86/FCGR2B/IFNG/IL12A/CXCR3/LY86/CD8B/RIPK2/UBE2D1/TPD52/HLA-DQA1/MRPL3/CD80/WARS/CD79A/CCR1/LCK/HDAC9/IGSF6/BCL10/TRAT1/CAPG/CD3G/CD96/IL11/IL2RB/MAP4K1/KRT1
	E2F TARGETS	105	0.805846	3.155588	0.007716	MAD2L1/CDKN2A/BIRC5/CKS2/CKS1B/CCNE1/TK1/UBE2S/PTTG1/UBE2T/MYBL2/NME1/CCNB2/AURKB/PLK1/DEPDC1/KPNA2/CDC20/RRM2/CENPM/CDKN3/CDK1/PLK4/AURKA/PCNA/SNRPB/KIF2C/SPC25/TRIP13/JPT1/ASF1B/ORC6/H2AFX/TOP2A/MELK/RNASEH2A/TACC3/CDCA8/DLGAP5/KIF4A/DCTPP1/SPC24/RFC3/CENPE/HMMR/RAD51AP1/DIAPH3/STMN1/POP7/BUB1B/DCK/MTHFD2/RPA3/GINS1/SPAG5/RACGAP1/KIF22/GINS4/DDX39A/DSCC1/CDC25A/KIF18B/RAN/E2F8/RFC2/TUBG1/SLBP/BRCA2/HMGB3/SUV39H1/CHEK1/PRIM2/GINS3/ESPL1/SMC4/MXD3
	G2M CHECKPOINT	104	0.759634	2.975861	0.007716	MAD2L1/CCNA2/UBE2C/BIRC5/CKS2/CKS1B/UBE2S/PTTG1/MYBL2/PBK/CCNB2/AURKB/PLK1/KPNA2/CDC20/CENPA/CDKN3/TTK/CDK1/PLK4/NEK2/AURKA/GINS2/KIF2C/JPT1/ORC6/H2AFX/CDC45/TOP2A/TROAP/TACC3/CDC6/SNRPD1/TPX2/KIF4A/NUSAP1/CENPE/HMMR/NDC80/STMN1/BUB1/EXO1/DTYMK/KIF23/TRAIP/PRC1/RACGAP1/KIF22/E2F1/DDX39A/CDC25A/POLQ/KIF15/FBXO5/RAD54L/KNL1/KIF11/BRCA2/HMGB3/E2F2/SUV39H1/CHEK1/CENPF/PRIM2/ESPL1/SMC4/ODC1/CCNF/STIL/SMC2/CDC7/MCM6/HIST1H2BK/EZH2/MCM2

Supplementary Table 5 continued. The Gene Set Enrichment Analysis (GSEA) of hub genes.

	Description	setSize	enrichmentScore	NES	p.adjust	core_enrichment
FANCD2	G2M CHECKPOINT	104	0.901015	3.369604	0.006028	MYBL2/KIF15/TPX2/TOP2A/KIF2C/UBE2C/BIRC5/ESPL1/MAD2L1/HMMR/PBK/KIF4A/PLK1/TROAP/TTK/BUB1/CDC20/POLQ/NUSAP1/RACGAP1/CCNB2/AURKB/CENPA/MKI67/CCNA2/KNL1/CDK1/TACC3/TRAIP/PLK4/E2F2/CENPF/AURKA/KIF23/KIF11/BRCA2/NEK2/CDC45/NDC80/EXO1/CDC25A/E2F1/CKS1B/CDC6/UBE2S/PRC1/KPNA2/RAD54L/CKS2/CENPE/SMC2/STIL/CCNF/LMNB1/CDKN3/PTTG1/STMN1/EZH2/ORC6/GINS2/CDC7/FBXO5/MCM2/ODC1/NSD2/H2AFX/KIF22/MCM6/INCENP/SMC4/CHEK1/DDX39A/KIF20B/BARD1/DTYMK/CHAF1A/SUV39H1
	E2F TARGETS	105	0.889041	3.34287	0.006028	MYBL2/CDKN2A/DEPDC1/MELK/CCNE1/ASF1B/TOP2A/KIF2C/TRIP13/BIRC5/ESPL1/BUB1B/MAD2L1/HMMR/KIF4A/PLK1/CDC20/CIT/CDCA8/SPAG5/SPC24/RACGAP1/CCNB2/AURKB/RRM2/TK1/MKI67/KIF18B/DLGAP5/CDK1/TACC3/PLK4/GINS4/AURKA/BRCA2/E2F8/RFC3/DIAPH3/SPC25/CDC25A/CKS1B/TIMELESS/UBE2S/RAD51AP1/KPNA2/CKS2/CENPE/GINS1/LMNB1/CDKN3/PTTG1/STMN1/UBE2T/CENPM/EZH2/ORC6/ATAD2/MCM2/MCM4/NCAPD2/HELLS/RNASEH2A/PCNA/H2AFX/KIF22/MCM6/SMC4/CHEK1/DDX39A/BARD1/DSCC1/GINS3/TCF19/SUV39H1/RFC2/CSE1L/UNG/MSH2/SNRPB/PRIM2/HMGB3/RAN/DCLRE1B/JPT1/NME1/TUBG1/DCK/MTHFD2/DCTPP1/TUBB/PAICS/DEK/PA2G4/DONSON/SLBP
	MITOTIC SPINDLE	80	0.798921	2.888574	0.006028	KIF15/TPX2/TOP2A/KIF2C/BIRC5/ESPL1/KIF4A/PLK1/TTK/BUB1/ANLN/NUSAP1/RACGAP1/CCNB2/ECT2/DLGAP5/CDK1/CENPF/AURKA/KIF23/KIF11/BRCA2/NEK2/NDC80/PRC1/PIF1/CENPE/LMNB1/FBXO5/KIF22/INCENP/SMC4/KIF20B/CENPJ/SASS6
PKD2	KRAS SIGNALING UP	118	0.656511	2.270659	0.004293	MMP11/PRRX1/PLAU/TMEM158/ETV1/CFH/GFPT2/LIF/PLAT/SPARCL1/ADGRA2/TMEM176A/MMP9/LAPTM5/ITGB2/PCSK1N/TMEM176B/RGS16/EPB41L3/ENG/NRP1/TNFAIP3/IL2RG/APOD/MALL/EPHB2/IKZF1/PLAUR/WNT7A/MAFB/TFPI/AKAP12/TRIB2/KLF4/CXCL10/SPP1/BMP2/C3AR1/SPON1/ETV5/ADAMDEC1/LCP1/FCER1G/FLT4/GYPC/G0S2/TRAF1/DUSP6/CTSS/ADAM8/SOX9/PPP1R15A/MMD/IRF8

Supplementary Table 5 continued. The Gene Set Enrichment Analysis (GSEA) of hub genes.

	Description	setSize	enrichmentScore	NES	p.adjust	core_enrichment
PKD2	TNFA SIGNALING VIA NFKB	109	0.696773	2.395892	0.004293	SERPINE1/PLAU/FOSB/KLF2/ICAM1/GFPT2/LIF/EGR1/SLC2A3/FOS/ZFP36/DUSP1/EGR2/TNFAIP6/NR4A1/GEM/OLR1/CCL5/NR4A3/EGR3/TNFAIP3/LDLR/TNFAIP2/GADD45B/PLAUR/PLEK/NFAT5/CDKN1A/CCL2/KDM6B/KLF4/CXCL1/CXCL10/BMP2/SIK1/IL6ST/DUSP4/FOSL2/CCL4/CXCL11/IER3/GOS2/TRAF1/JUNB/F3/CD44/PPP1R15A/SERPINB2/RHOB/NR4A2/KLF9/SGK1/PTGER4/IFIT2/B4GALT5/MAFF/IER5/CXCL6/ETS2/PER1/BCL6/TAP1/TNFRSF9/SMAD3/ID2/PLPP3/IL1B/PTX3/SLC2A6/RNF19B/BIRC3/IFIH1
	INTERFERON GAMMA RESPONSE	107	0.628308	2.160028	0.004293	C1S/CFH/CXCL9/ICAM1/C1R/XAF1/TNFAIP6/OAS2/IL2RB/LATS2/CCL5/CSF2RB/LCP2/IFI44L/OAS3/HLA-DQA1/RSAD2/TNFAIP3/HLA-B/TNFAIP2/MX1/HELZ2/SLAMF7/CDKN1A/CCL2/STAT1/CXCL10/FAS/EPST11/IFIT3/CD38/PIM1/TAPBP/CXCL11/SELP/CD74/WARS/ST8SIA4/IRF8/ST3GAL5/IFI44/LY6E/CD86/LGALS3BP/IFIT2/FCGR1A/OASL/EIF2AK2/MYD88/IFI30/CFB/TAP1/IFIT1/CMPK2/B2M/HLA-DRB1/PML/IFIH1/TXNIP/IFI27/HLA-G/JAK2/TRIM14
TBRG1	ALLOGRAFT REJECTION	120	0.489708	1.924057	0.008729	IL18/THY1/LIF/CD74/HLA-DOA/HLA-DMA/HLA-DQA1/C2/HLA-DRA/LTB/IL2RG/FAS/ELF4/PRKCB/CD47/PRKCG/B2M/CD3E/LY75/ICAM1/INHBB/TAP1/TAPBP/IL2RB/HDAC9/CD2/IL16/CCL5/GZMA/FYB1/CD96/CD4/JAK2/CXCL9/IL15/STAB1/CD7/CCL4/ITGAL/HLA-DOB/IGSF6/IKBKB/HLA-G/ITGB2/LYN/TNF/IL12A/SPI1/PTPRC/CRTAM/CD8A/PRF1/CCL22/WAS/LCP2/CTSS/CD3D/FASLG/CXCR3
	TNFA SIGNALING VIA NFKB	109	0.549517	2.128181	0.008729	BIRC3/IL18/CCND1/FOS/FOSB/LIF/CCL20/GADD45B/EGR1/CEBPD/EDN1/JUNB/SGK1/CCNL1/NR4A1/NFAT5/ZFP36/F3/IRF1/KLF2/TNFAIP2/IFIT2/CLCF1/SMAD3/ETS2/DUSP1/ICAM1/TAP1/LAMB3/MAFF/SERPINB2/PLAU/TRIB1/EGR3/BTG2/CCL5/TRAF1/IL6ST/CCL4/BTG3/TRIP10/TNFAIP3/IER3/TIPARP/EGR2/BMP2/TNF
	INTERFERON GAMMA RESPONSE	107	0.524759	2.03116	0.008729	CFB/XAF1/CD74/HLA-DMA/HLA-DQA1/IFITM3/HLA-DRB1/MX2/RTP4/PSMB8/IFI27/PSMB9/IRF1/IDO1/IFIT3/IFIT1/LY6E/FAS/TNFAIP2/IFIT2/EPST11/B2M/ZBP1/TXNIP/ICAM1/TAP1/TAPBP/IL2RB/PML/TNFSF10/ITGB7/HLA-B/CCL5/CASP8/GZMA/SLC25A28/JAK2/C1R/CXCL9/IL15/NMI/SECTM1/MX1/HLA-G/TNFAIP3/UBE2L6/C1S/PARP12

Supplementary Table 5 continued. The Gene Set Enrichment Analysis (GSEA) of hub genes.

	Description	setSize	enrichmentScore	NES	p.adjust	core_enrichment
DOCK5	TNFA SIGNALING VIA NFKB	109	0.558475	2.319462	0.007567	CD44/CCND1/FOSB/FOS/BIRC3/LAMB3/ TNFAIP2/IL18/NFAT5/LDLR/EGR3/KLF2/EGR1/ ZFP36/KLF9/BCL6/SIK1/SMAD3/DUSP1/ NR4A1/ETS2/IL6ST/SGK1/BTG2/CEBPD/ GADD45B/DUSP4/PER1/KLF4/IRF1/EDN1/ TRIP10/ICAM1/NR4A2/F3/TRAFF1/SLC2A3/ RHOB/FOSL2/IFIT2/STAT5A/CDKN1A/OLR1/ KYNU/PLAU/LIF/TNFAIP3/CXCL1/MAFF/EGR2/ JUNB/GFPT2/RIPK2/IL1B/RNF19B/F2RL1/ CXCL6/GOS2/PPP1R15A/PLEK/IER5/ICOSLG/ TNFAIP8/TRIB1/MAP2K3
	INFLAMMATORY RESPONSE	104	0.465585	1.916731	0.007567	SLC7A2/CD82/GPR132/STAB1/IL18/LDLR/ TNFSF15/TAPBP/P2RX7/CYBB/PTAFR/BTG2/ CLEC5A/TPBG/SLC7A1/MET/AHR/RASGRP1/ IL2RB/IRF1/SGMS2/EDN1/LYN/ICAM1/ GABBR1/F3/TNFSF10/ITGB8/C3AR1/APLNR/ LCP2/CDKN1A/OLR1/AQP9/LIF/RGS16/CCL22/ RGS1/SELE/RTP4/RIPK2/IL1B/ITGA5/CXCL6/ PCDH7/CD14/CCR7/SLC11A2/ICOSLG
	UV RESPONSE DN	62	0.584505	2.210784	0.007567	CELF2/MGLL/RUNX1/IRS1/DLC1/RBPMS/LDLR/ MT1E/SYNE1/SMAD3/PTPN21/DUSP1/GCNT1/ PTPRM/VLDLR/SIPA1L1/CAV1/SLC7A1/MET/ FHL2/PDGFRB/RND3/EFEMP1/F3/NRP1/ ANXA2/APBB2/PRDM2/PPARG

References:

- Siegel RL, Miller KD, Jemal A: Cancer statistics, 2019. *Cancer J Clin*, 2019; 69: 7–34
- Servant N, Roméjon J, Gestraud P et al: Bioinformatics for precision medicine in oncology: Principles and application to the SHIVA clinical trial. *Front Genet*, 2014; 5: 152
- Langfelder P, Horvath S: WGCNA: An R package for weighted correlation network analysis. *BMC Bioinformatics*, 2008; 9: 559
- Zhou Z, Cheng Y, Jiang Y et al: Ten hub genes associated with progression and prognosis of pancreatic carcinoma identified by co-expression analysis. *Int J Biol Sci*, 2018; 14: 124–36
- Zhou XG, Huang XL, Liang SY et al: Identifying miRNA and gene modules of colon cancer associated with pathological stage by weighted gene co-expression network analysis. *Oncotargets Ther*, 2018; 11: 2815–30
- Li N, Zhan X: Identification of clinical trait-related lncRNA and mRNA biomarkers with weighted gene co-expression network analysis as useful tool for personalized medicine in ovarian cancer. *EPMA J*, 2019; 10: 273–90
- Zhao Q, Fan C: A novel risk score system for assessment of ovarian cancer based on co-expression network analysis and expression level of five lncRNAs. *BMC Med Genet*, 2019; 20: 103
- Chen Y, Bi F, An Y et al: Identification of pathological grade and prognosis-associated lncRNA for ovarian cancer. *J Cell Biochem*, 2019; 120: 14444–54
- Chen Y, Bi F, An Y et al: Coexpression network analysis identified Kruppel-like factor 6 (KLF6) association with chemosensitivity in ovarian cancer. *J Cell Biochem*, 2018
- Liu J, Li S, Liang J et al: ITLNI identified by comprehensive bioinformatic analysis as a hub candidate biological target in human epithelial ovarian cancer. *Cancer Manag Res*, 2019; 11: 2379–92
- Mok SC, Bonome T, Vathipadiekal V et al: A gene signature predictive for outcome in advanced ovarian cancer identifies a survival factor: Microfibril-associated glycoprotein 2. *Cancer Cell*, 2009; 16: 521–32
- King ER, Tung CS, Tsang YT et al: The anterior gradient homolog 3 (AGR3) gene is associated with differentiation and survival in ovarian cancer. *Am J Surg Pathol*, 2011; 35: 904–12
- Yeung TL, Leung CS, Wong KK et al: ELF3 is a negative regulator of epithelial-mesenchymal transition in ovarian cancer cells. *Oncotarget*, 2017; 8: 16951–63
- Tone AA, Virtanen C, Shaw PA et al: Decreased progesterone receptor isoform expression in luteal phase fallopian tube epithelium and high-grade serous carcinoma. *Endocr Relat Cancer*, 2011; 18: 221–34
- Tung CS, Mok SC, Tsang YT et al: PAX2 expression in low malignant potential ovarian tumors and low-grade ovarian serous carcinomas. *Mod Pathol*, 2009; 22: 1243–50
- Carithers LJ, Ardlie K, Barcus M et al: A novel approach to high-quality post-mortem tissue procurement: The GTEx project. *Biopreserv Biobank*, 2015; 13: 311–19
- Mounir M, Lucchetta M, Silva TC et al: New functionalities in the TCGAbiolinks package for the study and integration of cancer data from GDC and GTEx. *PLoS Comput Biol*, 2019; 15: e1006701
- Gautier L, Cope L, Bolstad BM et al: Affy-analysis of Affymetrix GeneChip data at the probe level. *Bioinformatics*, 2004; 20: 307–15
- Leek JT, Johnson WE, Parker HS et al: The sva package for removing batch effects and other unwanted variation in high-throughput experiments. *Bioinformatics*, 2012; 28: 882–83
- Ritchie ME, Phipson B, Wu D et al: Limma powers differential expression analyses for RNA-sequencing and microarray studies. *Nucleic Acids Res*, 2015; 43: e47
- Yu G, Wang LG, Han Y et al: ClusterProfiler: An R package for comparing biological themes among gene clusters. *OMICS*, 2012; 16: 284–87
- Gladhaug IP, Westgaard A, Schjolberg AR et al: Spindle proteins in resected pancreatic head adenocarcinomas: BubR1 is an independent prognostic factor in pancreatobiliary-type tumours. *Histopathology*, 2010; 56: 345–55

23. Genga KR, Filho FD, Ferreira FV et al: Proteins of the mitotic checkpoint and spindle are related to chromosomal instability and unfavourable prognosis in patients with myelodysplastic syndrome. *J Clin Pathol*, 2015; 68: 381–87
24. Choi JW, Kim Y, Lee JH et al: High expression of spindle assembly checkpoint proteins *CDC20* and *MAD2* is associated with poor prognosis in urothelial bladder cancer. *Virchows Arch*, 2013; 463: 681–87
25. Nascimento AV, Singh A, Bousbaa H et al: *Mad2* checkpoint gene silencing using epidermal growth factor receptor-targeted chitosan nanoparticles in non-small cell lung cancer model. *Mol Pharm*, 2014; 11: 3515–27
26. Li L, Xu DB, Zhao XL et al: Combination analysis of *Bub1* and *Mad2* expression in endometrial cancer: Act as a prognostic factor in endometrial cancer. *Arch Gynecol Obstet*, 2013; 288: 155–65
27. Furlong F, Fitzpatrick P, O'Toole S et al: Low *MAD2* expression levels associate with reduced progression-free survival in patients with high-grade serous epithelial ovarian cancer. *J Pathol*, 2012; 226: 746–55
28. Nakano Y, Sumi T, Teramae M et al: Expression of the mitotic-arrest deficiency 2 is associated with chemotherapy resistance in ovarian serous adenocarcinoma. *Oncol Rep*, 2012; 28: 1200–4
29. Wang RH, Yu H, Deng CX: A requirement for breast-cancer-associated gene 1 (*BRCA1*) in the spindle checkpoint. *Proc Natl Acad Sci U S A*, 2004; 101: 17108–13
30. Torlakovic EE, Riddell R, Banerjee D et al: Canadian Association of Pathologists-Association canadienne des pathologistes National Standards Committee/Immunohistochemistry: Best practice recommendations for standardization of immunohistochemistry tests. *Am J Clin Pathol*, 2010; 133: 354–65
31. Balacescu O, Balacescu L, Tudoran O et al: Gene expression profiling reveals activation of the *FA/BRCA* pathway in advanced squamous cervical cancer with intrinsic resistance and therapy failure. *BMC Cancer*, 2014; 14: 246
32. van der Groep P, Hoelzel M, Buerger H et al: Loss of expression of *FANCD2* protein in sporadic and hereditary breast cancer. *Breast Cancer Res Treat*, 2008; 107: 41–47
33. Ozawa H, Iwatsuki M, Mimori K et al: *FANCD2* mRNA overexpression is a bona fide indicator of lymph node metastasis in human colorectal cancer. *Ann Surg Oncol*, 2010; 17: 2341–48
34. Han SS, Tompkins VS, Son DJ et al: *CDKN1A* and *FANCD2* are potential oncotargets in Burkitt lymphoma and multiple myeloma. *Exp Hematol Oncol*, 2015; 4: 9
35. Komatsu H, Masuda T, Iguchi T et al: Clinical significance of *FANCD2* gene expression and its association with tumor progression in hepatocellular carcinoma. *Anticancer Res*, 2017; 37: 1083–90
36. Moes-Sosnowska J, Rzepecka IK, Chodzynska J et al: Clinical importance of *FANCD2*, *BRIP1*, *BRCA1*, *BRCA2* and *FANCF* expression in ovarian carcinomas. *Cancer Biol Ther*, 2019; 20: 843–54
37. Kais Z, Rondinelli B, Holmes A et al: *FANCD2* maintains fork stability in *BRCA1/2*-deficient tumors and promotes alternative end-joining DNA repair. *Cell Rep*, 2016; 15: 2488–99